Extreme sea level implications of 1.5 °C, 2.0 °C, and 2.5 °C temperature stabilization targets in the 21st and 22nd centuries

Environmental Research Letters

LETTER

Extreme sea level implications of 1.5 °C, 2.0 °C, and 2.5 °C temperature stabilization targets in the 21st and 22nd centuries

D J Rasmussen[1,7], Klaus Bittermann[2], Maya K Buchanan[1,6], Scott Kulp[3], Benjamin H Strauss[3], Robert E Kopp[5] and Michael Oppenheimer[1,4]

1 Woodrow Wilson School of Public & International Affairs, Princeton University, Princeton, NJ, United States of America
2 Department of Earth and Ocean Sciences, Tufts University, Medford, MA, USA and Potsdam Institute for Climate Impact Research, Potsdam, Germany
3 Climate Central, Princeton, NJ, United States of America
4 Department of Geosciences, Princeton University, Princeton, NJ, United States of America
5 Department of Earth & Planetary Sciences and Institute of Earth, Ocean, & Atmospheric Sciences, Rutgers University, New Brunswick, NJ, United States of America
6 ICF International (Climate Adaptation and Resilience), New York, NY, United States of America
7 Author to whom any correspondence should be addressed.

E-mail: dj.rasmussen@princeton.edu

Keywords: sea level rise, coastal flooding, climate change impacts, paris agreement, IPCC, extreme sea levels

Supplementary material for this article is available online

OPEN ACCESS

RECEIVED
21 October 2017

REVISED
31 January 2018

ACCEPTED FOR PUBLICATION
2 February 2018

PUBLISHED
15 March 2018

Abstract

Sea-level rise (SLR) is magnifying the frequency and severity of extreme sea levels (ESLs) that can cause coastal flooding. The rate and amount of global mean sea-level (GMSL) rise is a function of the trajectory of global mean surface temperature (GMST). Therefore, temperature stabilization targets (e.g. 1.5 °C and 2.0 °C of warming above pre-industrial levels, as from the Paris Agreement) have important implications for coastal flood risk. Here, we assess, in a global network of tide gauges, the differences in the expected frequencies of ESLs between scenarios that stabilize GMST warming at 1.5 °C, 2.0 °C, and 2.5 °C above pre-industrial levels. We employ probabilistic, localized SLR projections and long-term hourly tide gauge records to estimate the expected frequencies of historical and future ESLs for the 21st and 22nd centuries. By 2100, under 1.5 °C, 2.0 °C, and 2.5 °C GMST stabilization, the median GMSL is projected to rise 48 cm (90% probability of 28–82 cm), 56 cm (28–96 cm), and 58 cm (37–93 cm), respectively. As an independent comparison, a semi-empirical sea level model calibrated to temperature and GMSL over the past two millennia estimates median GMSL rise within 7–8 cm of these projections. By 2150, relative to the 2.0 °C scenario and based on median sea level projections, GMST stabilization of 1.5 °C spares the inundation of lands currently home to about 5 million people, including 60 000 individuals currently residing in Small Island Developing States. We quantify projected changes to the expected frequency of historical 10-, 100-, and 500-year ESL events using frequency amplification factors that incorporate uncertainty in both local SLR and historical return periods of ESLs. By 2150, relative to a 2.0 °C scenario, the reduction in the frequency amplification of the historical 100 year ESL event arising from a 1.5 °C GMST stabilization is greatest in the eastern United States, with ESL event frequency amplification being reduced by about half at most tide gauges. In general, smaller reductions are projected for Small Island Developing States.

1. Introduction

Extreme sea levels (ESLs) are defined as the combined height of the astronomical tide and storm surge (i.e. the storm tide) and mean sea level. ESLs can cause coastal floods that threaten life and property when flood defenses are over-topped. Rising mean sea levels are already magnifying the frequency and severity of ESLs that lead to coastal floods (Buchanan *et al* 2017, Sweet and Park 2014) and, by the end of the

century, coastal flooding may be among the costliest impacts of climate change in some regions (Hsiang *et al* 2017, Diaz 2016, Hinkel *et al* 2014). Sea-level rise (SLR) is expected to permanently inundate low-lying geographic areas (Marzeion and Levermann 2014, Strauss *et al* 2015), but these locations will first experience decreases in the return periods of ESL events and associated coastal floods (e.g. Hunter 2012, Sweet and Park 2014).

The rate of global mean sea-level (GMSL) rise depends on the trajectory of global mean surface temperature (GMST; Rahmstorf 2007, Kopp *et al* 2016a, Vermeer and Rahmstorf 2009), with the long-term committed amount of GMSL largely determined by the stabilized level of GMST (Levermann *et al* 2013). Thus, the management of GMST has important implications for regulating future GMSLs (Schaeffer *et al* 2012), and consequently the frequency and severity of ESLs and coastal floods. However, GMST stabilization does not imply stabilization of all climate variables. Under stabilized GMST, GMSL is expected to continue to rise for centuries, due to the long residence time of anthropogenic CO_2, the thermal inertia of the ocean, and the slow response of large ice sheets to forcing (Clark *et al* 2016, Levermann *et al* 2013, Held *et al* 2010). For instance, Schaeffer *et al* (2012) found that a 2.0 °C GMST stabilization would lead to a GMSL rise (relative to 2000) of 0.8 m by 2100 and >2.5 m by 2300, but if the GMST increase were held below 1.5 °C, GMSL rise at the end of the 23rd century would be limited to ~1.5 m. These findings suggest that selection of climate policy goals could have critical long-term consequences for the impacts of future SLR and coastal floods (Clark *et al* 2016).

The Paris Agreement seeks to stabilize GMST by limiting warming to 'well below 2.0 °C above pre-industrial levels' and to further pursue efforts to 'limit the temperature increase to 1.5 °C above pre-industrial levels' (UNFCCC 2015a). However, a recent literature review under the United Nations Framework Convention on Climate Change (UNFCCC) found the notion that 'up to 2.0 °C of warming is considered safe, is inadequate' and that 'limiting global warming to below 1.5 °C would come with several advantages' (UNFCCC 2015b). The advantages and disadvantages of each GMST target as they relate to coastal floods and ESLs have not been quantified. This is critical, as >625 million people currently live in coastal zones with <10 m of elevation, and population growth is expected in these areas (Neumann *et al* 2015). Examining the short- and long-term ESL implications of 1.5 °C and 2.0 °C GMST stabilization scenarios, as others have recently done for other climate impacts (e.g. Schleussner *et al* 2016a, 2016b, Mitchell *et al* 2017, Mohammed *et al* 2017), may better inform the policy debate regarding the selection of GMST goals.

In this study, we employ probabilistic, localized SLR projections to assess differences in the frequency of ESLs across 1.5 °C, 2.0 °C, and 2.5 °C GMST stabilization scenarios at a global network of 194 tide gauges (section 2.1). We use long-term hourly tide gauge records and extreme value theory to estimate present and future return periods of ESL events (section 2.4.1). We extend our analysis through the 22nd century to account for continuing SLR in order to inform multi-century planning and infrastructure investments. Lastly, we assess differences in the exposure of current populations to future SLR under 1.5 °C, 2.0 °C, and 2.5 °C GMST stabilizations (section 3.2). Unlike deterministic or median estimates, the use of probabilistic projections allows for the characterization of uncertainty, which is important for risk management.

Various approaches have been used to project GMSL under GMST targets. For instance, Jevrejeva *et al* (2016) estimate future local SLR under a GMST increase of 2 °C using a representative concentration pathway (RCP) 8.5 GMST trajectory that passes through 2 °C of warming by mid-century, but this approach likely underestimates SLR relative to a scenario that achieves 2 °C GMST stabilization by 2100 as it neglects the time-lagged, integrated response of the ocean and cryosphere to warming (Clark *et al* 2016). More generally, studies that condition future ESL or flood projections on the RCPs may be insufficient for assessing the costs and benefits of climate policy scenarios, such as GMST stabilization targets (e.g. Section 13.7.2.2 of Church *et al* 2013, Buchanan *et al* 2017, Hunter 2012, Tebaldi *et al* 2012). The RCPs are designed to be representative of a range of emissions scenarios that result in prescribed anthropogenic radiative forcings by 2100 relative to pre-industrial conditions (e.g. 8.5 $W m^{-2}$ for RCP8.5). They are not representative of a specific emissions trajectory, climate policy (e.g. GMST target), or socioeconomic and technological change (Moss *et al* 2010, van Vuuren *et al* 2011). Recently, Jackson *et al* (2018) produced probabilistic, localized SLR projections under 1.5 °C and 2.0 °C GMST targets, but did not assess ESLs or consider sea-level change after 2100, the latter being necessary for evaluating the effects of GMST stabilization.

Semi-empirical sea level (SESL) models (Rahmstorf *et al* 2012) can estimate future GMSL rise under various GMST scenarios (e.g. Schaeffer *et al* 2012, Bittermann *et al* 2017). Unlike their process-based counterparts (e.g. Kopp *et al* 2014), SESL models do not explicitly model individual physical components of sea-level change. They are calibrated over a historical period using the observed statistical relationship between GMSL and a climate parameter (such as GMST). Assuming these relationships hold in the future, SESL models project the rate of GMSL change conditional upon a GMST pathway (e.g. Rahmstorf 2007, Vermeer and Rahmstorf 2009, Kopp *et al* 2016a). However, SESL models do not produce estimates of local SLR, which are necessary for

local risk assessment and adaptation planning because local SLR can substantially differ from the global mean (Milne *et al* 2009).

2. Methods

We project probabilistic global and local sea level conditional on GMST stabilization at 1.5 °C, 2.0 °C, and 2.5 °C using the component-based, local sea level projection framework from Kopp *et al* (2014, henceforth K14). We compare the GMSL projections from the K14 framework to those from the SESL model of Kopp *et al* (2016a) and Bittermann *et al* (2017). While SESL models cannot produce local projections of SLR, they can serve as a reference point for evaluating the consistency of process-based projections with historical temperature-GMSL relationships. The flow and sources of information used to construct the local SLR and GMSL projections using the K14 method is depicted in figure S-1(*a*), while the flow of information used to generate the SESL projections is provided in figure S-1(*b*). Local SLR projections from the K14 approach are combined with historical distributions of ESL events to estimate future return periods of historical ESL events (figure S-1(*a*)), similar to the approaches by Buchanan *et al* (2017, 2016) and Wahl *et al* (2017).

2.1. Component-based model approach: global and local sea-level rise projections

Sea-level change does not occur uniformly. Dynamic ocean processes (Levermann *et al* 2005), changes to temperature and salinity (i.e. steric processes), and changes in the Earth's rotation and gravitational field associated with water-mass redistribution (e.g. land-ice melt; Mitrovica *et al* 2011), as well as glacial isostatic adjustment (GIA; Farrell and Clark 1976) and other drivers of vertical land motion cause local relative sea levels to differ from the global mean. We model local relative sea level using the K14 framework, but make modifications to accommodate the stratification of atmosphere–ocean general circulation models (AOGCMs) and RCPs into groups that meet GMST stabilization targets (see section 2.2). AOGCM output from the Coupled Model Intercomparison Project (CMIP) Phase 5 archive (Taylor *et al* 2012) forced with the RCPs (to 2100) and their extensions (to 2300) are used directly for global mean thermal expansion (TE) and local ocean dynamics, and as a driver of a surface mass balance (SMB) model of glaciers and ice caps (GICs; Marzeion *et al* 2012). Antarctic ice sheet (AIS) and the Greenland ice sheet (GIS) contributions are estimated using a combination of the Intergovernmental Panel on Climate Change's (IPCC) Fifth Assessment Report (AR5) projections of ice sheet dynamics and SMB (table 13.5 in Church *et al* 2013) and expert elicitation of total ice sheet mass loss from Bamber and Aspinall (2013). As in AR5, ice sheet SMB contributions are represented as being dependent on the forcing scenario, while ice sheet dynamics are not. A spatiotemporal Gaussian process regression model is used with tide gauge data to estimate the long-term contribution from non-climatic factors such as tectonics, GIA, delta processes (e.g. sediment compaction), and human-induced subsidence. Changes in the rate of human-induced subsidence are not considered. Global mean land water storage effects are modeled using relationships between population and groundwater removal and impoundment (Kopp *et al* 2014). To generate probability distributions of global and local mean sea level for each GMST scenario at tide gauges (table S-1), we use 10 000 Latin hypercube samples of probability distributions of individual sea level component contributions.

2.2. Approximating global temperature stabilization with RCPs

The RCP-driven experiments in the CMIP5 archive are not designed to inform the assessment of climate impacts from incremental temperature changes. As such, we construct alternative ensembles for 1.5 °C, 2.0 °C, and 2.5 °C scenarios using CMIP5 output filtered according to each AOGCM's 2100 GMST. Specifically, we create ensembles for 1.5 °C, 2.0 °C, and 2.5 °C scenarios with AOGCMs that have a 21st century GMST increase (19 year running average) of 1.5 °C, 2.0 °C, and 2.5 °C (±0.25 °C). For consistency with the K14 framework, which models 19 year running averages of SLR relative to 2000, GMST is anomalized to 1991–2009 and then shifted upward by 0.72 °C to account for warming since 1875–1900 (Hansen *et al* 2010, GISSTEMP Team 2017). Selection of the AOGCMs for each scenario ensemble is made irrespective of the AOGCM's RCP forcing. For model outputs that end in 2100, we extrapolate the 19 year running average GMST to 2100 based on the 2070–2090 trend. While we chose 2100 as the determining year for which AOGCMs are selected for each ensemble, it should be noted that Article 2 of the UNFCCC (UNFCCC 1992) does not require that GMST stabilization be achieved within a particular timeframe. The Paris Agreement likewise does not specify a timeframe for GMST stabilization, though its goal of bringing net greenhouse gas (GHG) emissions to zero in the second half of the 21st century implies a similar timeframe for stabilization. We make the assumption that AOGCM outputs that end at 2100 either stay within the range of the target ±0.25 °C or fall below by any amount (i.e. undershoot). For AOGCMs that have GMST output available after 2100, only those that undershoot the target are retained. However, we make an exception to this rule for the 2.5 °C scenario ensemble in order to include AOGCMs for generating post-2100 projections. For RCP4.5 and RCP6, GMST stabilization should not occur before 2150, when GHG concentrations stabilize (Meinshausen *et al* 2011b) and so SLR projections after 2100 may

not be representative of conditions under true GMST stabilization. The GMST trajectories and GMSL contributions from TE and glacial ice from selected CMIP5 models that are binned into 1.5 °C, 2.0 °C, and 2.5 °C GMST categories are shown in figures 1 and S-2, respectively. Table S-2 lists the AOGCMs employed in each GMST scenario ensemble and the sea-level components used. Given the paucity of CMIP5 output after 2100, the range of TE and GIC contributions to SLR in the 22nd century is likely underestimated relative to the 21st century. Total ice sheet contributions from AR5 are calculated for each GMST scenario by randomly sampling AIS and GIS ice sheet distribution for each RCP (table 13.5 in Church *et al* 2013) in proportion to the representation of each RCP in the groups of CMIP5 models selected for each GMST scenario[8].

2.3. GMSL rise projections from a SESL model

We generate estimates for GMSL for 2000–2200 using the SESL model from Kopp *et al* (2016a) and Bittermann *et al* (2017) driven with both GMST trajectories from CMIP5 models (figure 1) and GMST trajectories from the reduced-complexity climate model MAGICC6 (Meinshausen *et al* 2011a, as employed in Rasmussen *et al* 2016) for 2100 GMST targets of 1.5 °C, 2.0 °C, and 2.5 °C (±0.25 °C) (figure S-3). The MAGICC6 GMST trajectories are selected from all RCP-grouped projections using the same criteria as in section 2.2. The SESL model is calibrated to the common era temperature reconstruction from Mann *et al* (2009) and the sea level reconstruction of Kopp *et al* (2016a). The historical statistical relationship between temperature and the rate of sea-level change is assumed to be constant; not included are nonlinear physical processes or critical threshold events that could substantially contribute to SLR, such as ice sheet collapse (Kopp *et al* 2016b, Levermann *et al* 2013). Threshold behavior is partially incorporated in the K14 framework through expert assessments of future ice sheet melt contributions (Bamber and Aspinall 2013), which may be one reason why the K14 framework produces higher estimates in the upper tail of the SLR probability distribution.

2.4. Estimating the frequency of historical and future extreme sea level events

The heights of historical ESL events that result from tropical and extra-tropical cyclones, extreme astronomical tides, and other processes are recorded in sub-daily tide gauge observations. Extreme value theory can be used with these tide gauge measurements to estimate the historical return levels of ESL events, including events that occur less often, on average, than the length of the observational record. For example, one could use extreme value theory to estimate the height of the present-day 500 year (or 0.2% average annual probability) ESL event from a record that is <500 years in length. Assuming no non-linear relationships between SLR and ESL events and no change in the frequency and intensity of processes that cause ESLs (e.g. tropical and extra-tropical cyclones), the estimated return levels of historical ESL events can be combined with local SLR projections to estimate the return levels of future ESL events.

2.4.1. *Estimation of historical return levels of extreme sea levels*

Here, we use extreme value theory with daily maximum sea levels at tide gauges archived by the University of Hawaii Sea Level Center (see supplementary data; Caldwell *et al* 2015) to estimate historical return levels of ESL events. Specifically, we follow Tebaldi *et al* (2012) and Buchanan *et al* (2016, 2017) and employ a generalized Pareto distribution (GPD) and a peaks-over-threshold approach (Coles 2001b, 2001a). The GPD describes the probability of a given ESL height conditional on an exceedance of the GPD threshold. We use the 99th percentile of daily maximum sea levels as the GPD threshold, which is generally both above the highest seasonal tide and balances the bias-variance trade-off in the GPD parameter estimation (Tebaldi *et al* 2012). The number of annual exceedances of the GPD threshold is assumed to be Poisson distributed with mean λ. Tide gauge observations are detrended and referenced to mean higher high water (MHHW)[9] and the GPD parameters are estimated using the method of maximum likelihood (see supplementary data). Uncertainty in the GPD parameters is calculated from their estimated covariance matrix and is sampled using Latin hypercube sampling of 1000 normally distributed GPD parameter pairs. For a given tide gauge, the annual expected number of exceedances of ESL height z is given by $N(z)$:

$$N(z) = \begin{cases} \lambda\left(1 + \frac{\xi(z-\mu)}{\sigma}\right)^{-\frac{1}{\xi}} & \text{for} \quad \xi \neq 0 \\ \lambda \exp\left(-\frac{z-\mu}{\sigma}\right) & \text{for} \quad \xi = 0 \end{cases} \tag{1}$$

where the shape parameter (ξ) governs the curvature and upward statistical limit of the ESL event return curve, the scale parameter (σ) characterizes the variability in the exceedances caused by the combination of tides and storm surges, and the location parameter (μ) is the threshold water-level above which return levels are estimated with the GPD, here the 99th percentile of daily maximum sea levels. Meteorological and hydrodynamic differences between sites give rise

[8] For example, the 1.5 °C GMST employs 12 CMIP5 models from RCP2.6 and 2 from RCP4.5, so 86% of the samples aredrawn from the RCP2.6 distribution and 14% are drawn from the RCP4.5 distribution (supplementary information (SI), table S-2 available at stacks.iop.org/ERL/13/034040/mmedia).

[9] Here defined as the average level of high tide over the last 19-years in each tide gauge record, which is different from the current US National Tidal Datum Epoch of 1983–2001.

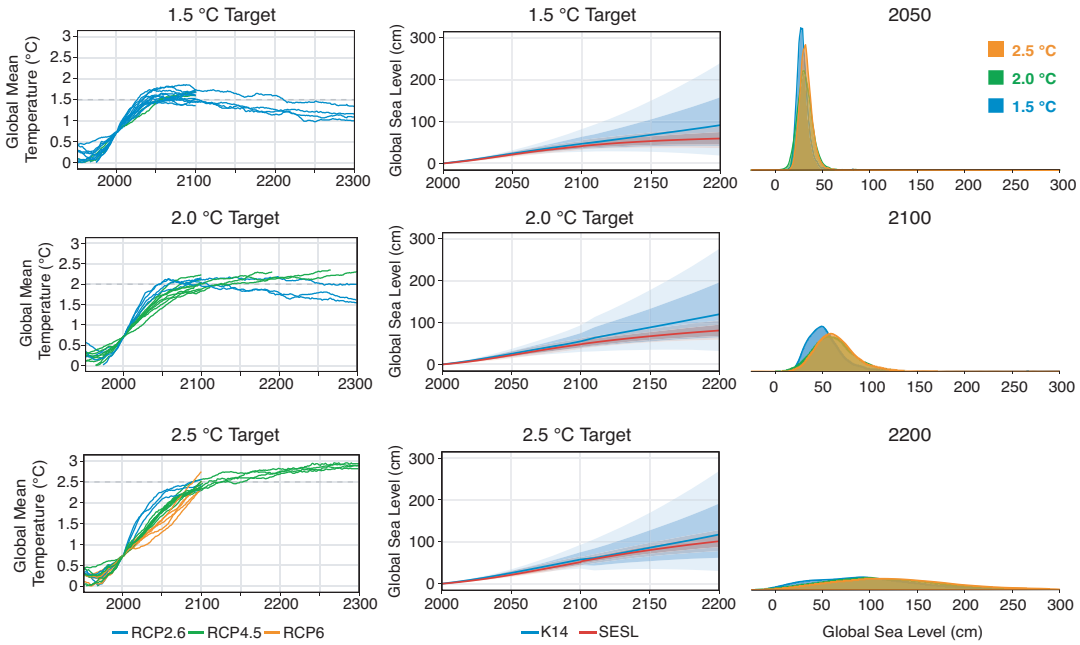

Figure 1. Left column: GMST trajectories from CMIP5 models (1950–2300) that have a 19 year running average 2100 GMST of 1.5 °C, 2.0 °C, and 2.5 °C ±0.25 °C (relative to 1875–1900; blue = RCP2.6, green = RCP4.5, orange = RCP6). GMST is anomalized to 1991–2009 and shifted up by 0.72 °C to account for warming since 1875–1900 (Hansen *et al* 2010, GISSTEMP Team 2017). Table S-2 (SI) lists the CMIP5 models used for each GMST target. Middle column: GMSL rise (cm; relative to 2000) from the methodology of Kopp *et al* (2014) (K14; blue), using CMIP5 temperature trajectories from the left column, and a SESL model from Kopp *et al* (2016a) (red). Temperature trajectories that drive the SESL model are shown in the left column. The thick line is the 50th percentile, heavy shading is the 17/83rd percentile, and light shading is the 5/95th percentile. Right column: probability distributions of projected 2050, 2100, and 2200 global mean sea-level rise for GMST stabilization targets using the Kopp *et al* (2014) framework (blue = 1.5 °C, green = 2.0 °C, orange = 2.5 °C).

to differences in the shape parameter (ξ). ESL frequency distributions with $\xi > 0$ are 'heavy tailed', due to a higher frequency of events with extreme high water (e.g. tropical and extra-tropical cyclones). Distributions with $\xi < 0$ are 'thin tailed' and have a statistical upper bound on extreme high water levels. Events that occur between λ and 182.6/year (i.e. exceeding MHHW half of the days per year) are modeled with a Gumbel distribution, as they are outside of the support of the GPD. Note that ESL events at tide gauges are not referred to as floods as the occurrence of an actual flood depends on the level of coastal flood protection, terrain, infrastructure, and other local factors.

2.4.2. *Extreme sea level event frequency amplification factors*

The frequency amplification factor (AF) quantifies the increase in the expected frequency of historical ESL events (e.g. the 100 year ESL event) due to SLR (Buchanan *et al* 2017, Hunter 2012, Church *et al* 2013). Due to variation in the local storm climate and hydrodynamics, the height of ESL event return levels are unique to each location (SI, figure S-4). The calculation of the expected AF includes both the uncertainty in the estimates of the return periods of historical ESL events and uncertainty in SLR projections. Following Buchanan *et al* (2017), we define the expected ESL event frequency amplification factor AF(z) for ESL events with height z as the ratio of the expected number of ESL events after including uncertain SLR to the historical expected number of ESL events:

$$\mathrm{AF}(z) = \frac{E\left[N\left(z-\delta\right)\right]}{N\left(z\right)} \qquad (2)$$

where $N(z–\delta)$ is the annual expected number of exceedances of ESL height z after including SLR (δ), $E[\cdot]$ is the expectation operator applied to the full probability distribution of SLR projections, and $N(z)$ is the historical annual expected number of exceedances of ESL height z.

2.4.3. *Assessment of population exposure*

Following the methods used in Kopp *et al* (2017), we assess the current population living on land exposed to future permanent inundation from GMSL under each GMST stabilization scenario. We emphasize that this is not a literal measure of future population exposure—which will depend upon population growth, the dynamic response of the population to rising sea levels, and coastal protective measures taken—but is instead intended to index the relevance of SLR to current economic development and cultural heritage under different GMST stabilizations. We use a 1 arc-sec SRTM 3.0 digital elevation model from NASA (NASA JPL 2013) referenced to local MHHW levels for the year 2000 and this study's local SLR projection grids. Projected inundation areas are intersected with

Table 1. GMSL projections. All values are cm above 2000 CE baseline. AIS = Antarctic ice sheet, GIS = Greenland ice sheet; TE = thermal expansion; GIC = glaciers and ice caps; LWS = land water storage. AIS and GIS ice sheet distributions for each RCP from the Intergovernmental Panel on Climate Change's Fifth Assessment Report (Church *et al* 2013) are randomly sampled in proportion to the RCP representation in the CMIP5 model filtering (table S-2). K16: SESL model from Kopp *et al* (2016a) driven with GMST trajectories from MAGICC (see SI figure S-3) and CMIP5 GMST trajectories (see figure 1); J18: Jackson *et al* (2018), S16: Schleussner *et al* (2016a).

	1.5 °C			2.0 °C			2.5 °C		
cm	50	17–83	5–95	50	17–83	5–95	50	17–83	5–95
2100—Components									
AIS	6	−4–17	−8–35	6	−5–17	−8–34	6	−5–16	−8–34
GIS	7	4–12	3–19	8	4–14	2–22	8	4–15	2–22
TE	19	14–23	10–27	25	15–34	7–42	26	20–31	16–35
GIC	11	8–13	6–15	11	7–16	2–21	13	11–15	9–17
LWS	5	3–7	2–8	5	3–7	2–8	5	3–7	2–8
Total	48	35–64	28–82	56	39–76	28–96	58	45–75	37–93
Projections by year									
2050	24	20–28	18–32	25	20–32	15–37	26	22–30	19–34
2070	34	27–41	24–50	38	28–48	21–58	38	32–47	27–55
2100	48	35–64	28–82	56	39–76	28–96	58	45–75	37–93
2150	69	42–107	28–151	88	50–133	25–181	86	54–126	35–171
2200	93	43–161	20–241	120	57–197	20–281	118	62–189	31–268
Other projections for 2100									
K16[a]	38	33–43	30–47	45	39–52	35–58	54	47–62	42–68
K16[b]	41	36–48	32–53	48	41–56	36–62	51	45–59	41–65
J18	44	30–58	20–67	50	35–64	24–74	–	–	–
S16	41	29–53	–	50	36–65	–	–	–	–
Other projections for 2200									
K16[a]	58	45–72	36–81	79	65–93	56–104	100	85–115	75–127
K16[b]	59	45–75	37–88	81	68–95	59–105	101	87–116	78–128

[a] SESL model driven with MAGICC6 GMST trajectories shown in SI figure S-3.

[b] SESL model driven with CMIP5 GMST trajectories shown in figure 1.

LandScan 2010 global population data on a 1 km × 1 km global grid (Bright *et al* 2011) and national boundary data (Hijmans *et al* 2012). For each GMST target, the current population on land at risk is assessed at the 5th, 50th, and 95th percentile local SLR projection. Further details are provided in the supplementary information of Kopp *et al* (2017).

3. Results

3.1. GMSL rise

The GMSL projections for each GMST target from the K14 and SESL method are shown in figure 1 and are tabulated along with the component contributions in table 1. For the K14 method, differences in median GMSL between 1.5 °C, 2.0 °C, and 2.5 °C GMST stabilization targets do not appear until after 2050, when the 1.5 °C scenario begins to separate from the 2.0 °C and 2.5 °C trajectories (table 1). The median GMST trajectories diverge earlier, around 2030 (figure S-3). This is consistent with the early to mid-century divergence in the radiative forcing pathways and this study's allocation of RCPs in the 1.5 °C (primarily RCP2.6), 2.0 °C (primarily RCP4.5), and 2.5 °C (primarily RCP4.5 and RCP6) scenarios (SI, table S-2). Median projections for 2100 GMSL under a 1.5 °C scenario are 48 cm, with a *very likely* range (90% probability) of 28–82 cm. An additional 8–10 cm of median GMSL rise is found for the 2.0 °C and 2.5 °C GMST scenarios, 56 cm (*very likely* 28–96 cm) and 58 cm (*very likely* 37–93 cm), respectively. Prior to mid-century, TE and GIC contributions account for more than half of GMSL projection uncertainty, but by 2100, ice sheet contributions dominate (SI, figure S-5). Other studies found similar GMSL results. Using the same framework, Kopp *et al* (2014) estimated median 2100 GMSL projections under RCP2.6 and RCP4.5 of 50 cm (*very likely* 29–82 cm) and 59 cm (*very likely* 36–93 cm), respectively. Jackson *et al* (2018) also employs the CMIP5 ensemble to estimate probabilistic local SLR projections for GMST stabilizations, but do not consider non-linear ice dynamics (e.g. Bamber and Aspinall 2013). Their median projections for 1.5 °C (44 cm; *very likely* 20–67 cm) and 2.0 °C (50 cm; *very likely* 24–74 cm) GMST stabilizations are within 4–6 cm of this study. Using a method that scales SLR component contributions as a function of GMST and ocean heat uptake (Perrette *et al* 2013), Schleussner *et al* (2016a) estimated a median 2100 GMSL for 1.5 °C and 2.0 °C scenarios, that is 6–7 cm lower than this study's K14 framework projections. (table 1).

Despite being warmer by a half-degree, the 2.5 °C GMSL projections largely overlap the 2.0 °C scenario (figure 1). Variation in the transient climate response and ocean heat uptake efficiency across CMIP5 models leads to weak correlation between TE and GMST ($r^2 = 0.10$; figure S-6; Kuhlbrodt and Gregory 2012, Raper *et al* 2002). As such, cooler models may produce more TE than warmer models, and vice versa. Ice sheet contributions are also similar between 2.0 °C and 2.5 °C scenarios (table 1). To test the sensitivity of model-RCP filtering to the choice of GMST stabilization, we additionally calculate GMSL under a 1.75 °C

Table 2. The current population (in millions) living on lands exposed to future permanent inundation from median (5th–95th percentile) local sea-level rise (SLR) projections. Population estimates are from 2010. The top five countries with the most exposure in 2150 are included in the table as well as United Nations defined SIDS.

Human population exposure under 2100 local SLR projections (millions)				
Region	Total Population	1.5 °C	2.0 °C	2.5 °C
World	6,836.42	46.12 (31.92–69.23)	48.76 (32.01–79.65)	50.35 (33.33–77.38)
China	1,330.20	11.70 (5.89–20.37)	12.75 (6.00–22.05)	13.26 (6.18–22.91)
Vietnam	89.55	6.57 (4.56–9.91)	6.96 (4.58–10.65)	7.16 (4.66–11.05)
Japan	126.66	4.44 (3.84–5.56)	4.62 (3.88–5.85)	4.69 (3.89–6.11)
Netherlands	16.78	4.71 (4.20–5.57)	4.86 (4.16–5.87)	4.85 (4.36–5.63)
Bangladesh	156.13	2.83 (1.98–4.33)	3.03 (2.05–4.77)	3.09 (2.13–4.92)
SIDS	62.08	0.40 (0.30–0.56)	0.42 (0.30–0.64)	0.43 (0.32–0.63)
Human population exposure under 2150 local SLR projections (millions)				
Region	Total Pop.	1.5 °C	2.0 °C	2.5 °C
World	6,836.42	56.05 (32.54–112.97)	61.84 (32.89–138.63)	62.27 (34.08–126.95)
China	1,330.20	14.46 (5.73–31.00)	16.92 (5.86–37.08)	16.58 (5.75–36.48)
Vietnam	89.55	7.60 (4.46–15.19)	8.47 (4.51–17.13)	8.33 (4.54–16.58)
Japan	126.66	4.92 (3.87–7.69)	5.40 (3.94–8.72)	5.35 (3.89–8.61)
Netherlands	16.78	5.06 (4.12–6.49)	5.18 (4.22–6.45)	5.28 (4.38–6.48)
Bangladesh	156.13	4.48 (2.58–9.78)	5.10 (2.67–11.95)	5.01 (2.82–11.15)
SIDS	62.08	0.46 (0.29–0.91)	0.52 (0.29–1.14)	0.52 (0.31–1.01)

and 2.25 °C GMST scenario. The median 2100 GMSL under the 1.75 °C scenario is 3 cm greater than the 1.5 °C scenario, and the 2.25 °C scenario is 1 cm less than the 2.0 °C scenario (table S-3), suggesting that GMST scenarios that are primarily represented by only one RCP (i.e. the 1.5 °C scenario) may be less sensitive to model filtering.

Agreement between central estimates from process-based and semi-empirical projections implies consistency with the observed statistical relationship between GMST and the rate of SLR used to calibrate the SESL model. Across scenarios, median 2100 GMSL projections from the SESL model driven with CMIP5 GMST trajectories are 7–8 cm lower than those from the K14 framework (figure 1 and table 1), but more disagreement exists between the processed-based and SESL projections when driven with the MAGICC GMST trajectories shown in SI, figure S-3 (median projection differences of 4–11 cm; table 1). These differences are smaller in magnitude relative to the differences in the median RCP2.6 and RCP4.5 projections from Kopp *et al* (2014) and the SESL projections from Kopp *et al* (2016a) (8–12 cm). After 2100, the differences between projections from the K14 framework and the SESL model become larger. Across scenarios, median 2200 GMSL projections from the K14 framework are higher by 34 cm (1.5 °C), 39 cm (2.0 °C) and 17 cm (2.5 °C) than those from the SESL model driven with CMIP5 GMST trajectories (figure 1 and table 1). These differences are largely attributed to the treatment of ice sheets in each approach. The K14 framework accounts for non-linearities in crossing threshold ice sheet behavior by drawing from AR5 and Bamber and Aspinall (2013), but the SESL model does not because these events are absent from the calibration period.

3.2. Population inundation

Under the median projected GMSL for a 2.0 °C GMST stabilization, lands currently home to about 60 million people are projected to be permanently submerged by 2150, including lands currently home to over half a million inhabitants of United Nations defined Small Island Developing States (SIDS). Aggregation of all SIDS can mask important risks. For instance, local SLR projections for 2150 under a 2.0 °C GMST stabilization place lands currently home to almost a quarter of the current population of the Marshall Islands at risk of being permanently submerged. In comparison to these totals, under the median projection for the 1.5 °C stabilization scenario, lands currently home to about 5 million people, including 60 000 in SIDS, avoid inundation (table 2), but little difference is found for the Marshall Islands.

3.3. Amplification of ESL events

We assess the effects of different GMST stabilizations on the frequency of ESL events by highlighting three cities: (1) New York, New York, USA, (2) Kushimoto, Wakayama, Japan, and (3) Cuxhaven, Lower Saxony, Germany (figure 2). Estimates of the historical 10-, 100-, and 500-year ESL events (expected frequency of 0.1/year, 0.01/year, and 0.002/year, respectively) and the future ESL frequency AF for all sites are provided in SI tables S-4 to S-6. Under 2.0 °C GMST stabilization, the 2100 median local SLR for New York City is 69 cm (*likely* 44–98 cm). In figure 2, median local SLR under the 2.0 °C scenario (SL_{50}) shifts the expected historic ESL event return curve to the right (i.e. N(z), the heavy gray curve, becomes N+SL_{50} 2.0 °C, the dashed green curve) and increases the expected annual number of historical 10 year ESL events from 0.1/year to ~10/year. However, when both the uncertainty in the GPD fit and the SLR projections are considered in the calculation of the projected future ESL event return curve (i.e. N_e 2.0 °C; the heavy green curve), the expected frequency of the current 10 year ESL event increases from 0.1/year to 36/year (i.e. 3/month, on average). GHG mitigation that

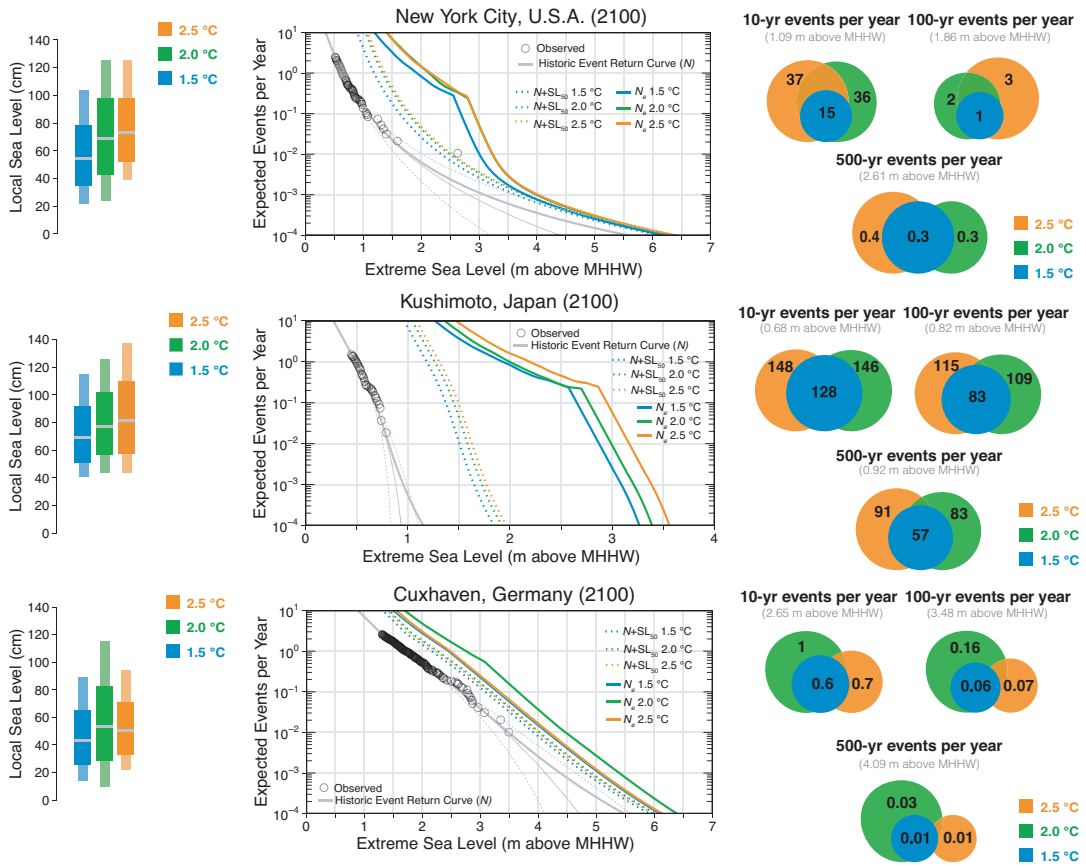

Figure 2. Top left: 2100 SLR (cm; relative to 2000) for New York City, USA, under 1.5 °C (blue), 2.0 °C (green), and 2.5 °C (orange) GMST stabilizations. Gray bars are median, heavy colors are 17/83 percentile and light shading is 5/95 percentile. Top middle: ESL event return curves for New York City indicating the relationship between the expected number of ESL events per year and ESL height (m above MHHW) for: 1) historical conditions (gray curves) and 2) year 2100 under both different GMST stabilizations (blue = 1.5 °C, green = 2.0 °C, orange = 2.5°C) and consideration of local SLR uncertainty (dotted curves consider median SLR only (i.e. a fixed offset from N, $N + SL_{50}$); solid curves (N_e) incorporate local SLR projection uncertainty by integrating across both the entire SLR probability distribution and GPD parameter uncertainty; blue, green, and orange colors are the 1.5 °C, 2.0 °C, 2.5 °C scenarios, respectively). The thick gray curve is the expected historical ESL height return curve (N) that incorporates the uncertainty in the GPD parameter fit, open gray circles are observed ESL events from the tide gauge record, and thin grey lines are the historical ESL height return curves for the 17/50/83 percentiles of the GPD parameter uncertainty range (dotted/solid/dotted lines, respectively). The shape of the N_e curve varies by location in part because both local SLR uncertainty and the shape of the historical return curve vary by location. Top right: the expected number of ESL events per year by historical return period for New York City for 2100 under 1.5 °C (blue), 2.0 °C (green), and 2.5 °C (orange) GMST stabilization. Second row: as for top row, but for Kushimoto, Japan. Third row: as for top row, but for Cuxhaven, Germany.

stabilizes GMST at 1.5 °C reduces projected median local SLR at New York City to 55 cm (*likely* 35–78 cm), and reduces the expected number of current 10 year ESL events by half (15/year). By 2150, the reduction in projected 10 year ESL events from the 2.0 °C to the 1.5 °C scenario is still ~50% (99/year reduced to 59/year; table S-4).

Note that the expected number of flood events and the appearance of kinks in the N_e curves in figure 2 are sensitive to the way that the high-end tail of the mean sea level distributions are constructed. For example, for sample sizes explored in this study (<99.9th percentile), this truncation plays an important role in setting the location of the kinks in N_e and for sufficiently heavy tailed distributions, N_e may not converge within this range. Discontinuities in the N_e curves can also arise at the transition between modeling flood events with two different distributions. Specifically, expected ESL frequencies between the historical frequency of the GPD threshold exceedance (i.e. λ) and 182.6 events per year are modeled with a Gumbel distribution and expected ESL frequencies greater than λ are modeled with a GPD (section 2.4.1). Note that because the uncertainty in local SLR varies by location, the distance between the N+SL_{50} and N_e curves also differs by location.

Sea-level rise will amplify the frequency of all ESL events, but depending on the shape of the GPD, the frequency of some ESL events may amplify more than others (Buchanan *et al* 2017). For example, by 2100 under a 2.0 °C and 1.5 °C GMST stabilization, respectively, median local SLR for Kushimoto, Japan is projected to be 79 cm (*likely* 58–103 cm) and 70 cm (*likely* 52–92 cm), increasing the respective number of historical 10 year ESL events from 0.1/year, on average, to 146/year (AF of 1462) and 128/year (AF of 1277), on average. However, for the same amount of local SLR, the historical number of expected 500 year

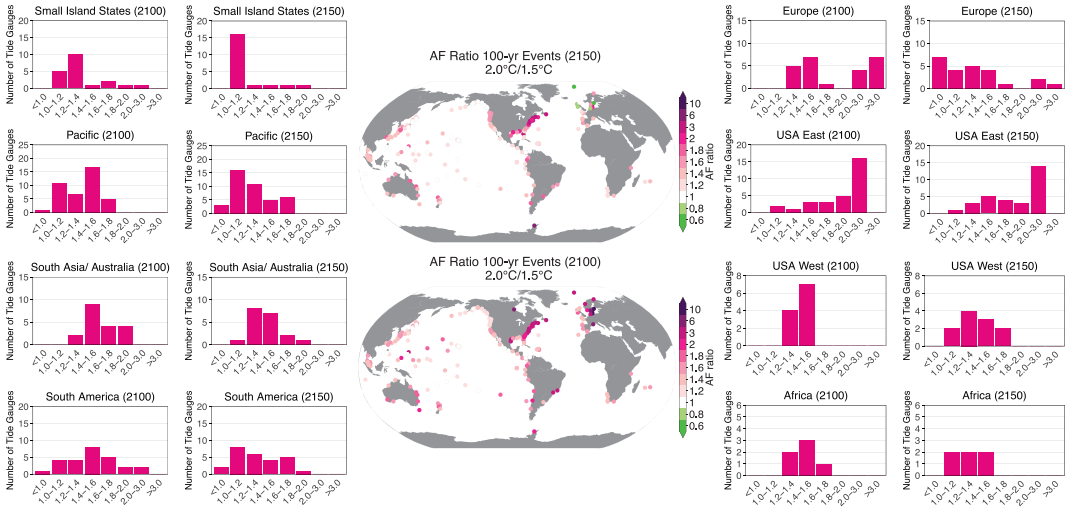

Figure 3. Maps: the ratio of ESL event AFs for historical 100 year ESL events between a 1.5 °C and 2.0 °C GMST stabilization target for the years 2150 (top) and 2100 (bottom). Larger 2.0 °C/1.5 °C AF ratios indicate where the historical 100 year ESL event occurs less often under 1.5 °C GMST stabilization than 2.0 °C GMST stabilization. Histograms: regionally binned ratios of 2.0 °C/1.5 °C expected AFs for the historical 100 year ESL event for 2100 and 2150. 'Small Island States' are United Nations defined Small Island Developing States. The list of tide gauges included in each region are given in table S-1 (SI).

ESL events for Kushimoto increases from 0.002/year to 83/year (2.0 °C; AF of 41479) and 57/year (1.5 °C; AF of 28 645). When the shape of the return curve is log-linear (as occurs when the shape parameter (ξ) is zero), ESL events amplify equally across return periods. For example, by 2100, under 1.5 °C, 2.0 °C, and 2.5 °C GMST stabilization, respectively, Cuxhaven, Germany is projected to have median local SLR of 43 cm (*likely* 26–65 cm), 53 cm (*likely* 29–82 cm) and 51 cm (*likely* 34–71 cm). The historical 500 year ESL event is projected to become as or more frequent than the historical 100 year ESL event for all scenarios: 0.01/year (1.5 °C; AF of 5.6), 0.03/year (2.0 °C; AF of 13.5), and 0.01/year (2.5 °C; AF of 6.5). Because the shape factor of the Cuxhaven GPD is close to zero, the historical 10 year ESL event also is projected to amplify similarly to the 500 year ESL event: 0.6/year (1.5 °C; AF of 5.6), 1.0/year (2.0 °C; AF of 13.5), and 0.7/year (2.5 °C; AF of 6.5). For some sites, including Cuxhaven, the AF for the 2.0 °C scenario may be greater than the AF for the 2.5 °C scenario. This can be partly attributed to higher SLR projections in the upper tail of the 2.0 °C probability distribution influencing the AF calculation.

We assess regional differences in 100 year ESL event frequency amplification between 2.0 °C and 1.5 °C GMST stabilization by binning ratios of 2.0 °C/1.5 °C expected AFs for 2100 and 2150 (figure 3). Bins on the right side of each graph become filled when there are decreases in the frequency of ESL events at regional groups of tide gauges from 1.5 °C over 2.0 °C GMST stabilization, while bins on the left side of each graph become filled when there are either no changes or increases in ESL event frequency at stations from 1.5 °C GMST over 2.0 °C GMST stabilization. In general, decreases in the frequency of ESL events from a 1.5 °C GMST stabilization grow as GMSL trajectories between scenarios separate from one another (table 1). By 2100 and 2150, substantial decreases in the frequency of ESL events from 1.5 °C GMST stabilization are expected in the East and Gulf Coasts of the United States, where ESL event amplification between GMST scenarios is reduced by roughly half. By 2150, smaller contributions from either local ocean dynamics or GICs in the 2.0 °C scenario attenuate SLR in parts of Europe, leading to lower median local SLR than from 1.5 °C GMST stabilization. Less local SLR in the 2.0 °C scenario causes ESL event frequencies to decrease, relative to the 1.5 °C scenario. We find small decreases or no change in ESL event frequency from achieving a 1.5 °C GMST stabilization over a 2.0 °C GMST stabilization at most tide gauges located in SIDS, as local SLR projections in these areas are similar between GMST scenarios (figure 3).

4. Discussion and conclusions

The Paris Agreement seeks to stabilize GMST by limiting warming to 'well below 2.0 °C above pre-industrial levels', but a recent literature review under the UNFCCC found the notion that 'up to 2.0 °C of warming is considered safe, is inadequate' and that 'limiting global warming to below 1.5 °C would come with several advantages' (UNFCCC 2015b). However, the location-specific increases in the frequency of ESLs illustrate the divergence between local and global perspectives on the question of what climate changes are 'dangerous'. The selection of a GMST target has important implications for long-term GMSL rise, ESLs, and consequently, coastal flooding. Assessing the distribution of impacts of incremental levels of warming

on ESLs is of relevance to >625 million people who currently reside in low-lying coastal areas (Neumann *et al* 2015) and are vulnerable to current and future ESL events. For countries without the economic and physical capacity to construct flood protection and flood-resilient infrastructure—including some recognized by the United Nations as SIDS—local SLR that results in permanent inundation and unmanageable flooding may threaten their existence (Wong *et al* 2014, Diaz 2016). The only feasible option for maintaining habitability for these locations may be the management of GMST through international climate accords, like the Paris Agreement, that govern the long-term committed rise in GMSL.

Only considering changes to the mean local sea level, we find that, under median projections, lands currently home to 5 million people will be spared from being permanently submerged by local mean sea levels by 2150 under a 1.5 °C GMST stabilization compared to local mean sea levels under the 2.0 °C case. This includes lands in SIDS currently home to 60 000 people (table 2). The effects of GMST stabilization on ESLs varies greatly by region and by historical return period (e.g. the 10 year versus the 100 year ESL event, etc). Globally, for the historical 100 year ESL event, we find that by 2100, the Eastern and Gulf coasts of the US and Europe could experience substantial benefits from a 1.5 °C GMST stabilization relative to a 2.0 °C GMST stabilization, with ESL frequency amplification being reduced by about half. However, while fractional reductions may appear substantial in some cases, small absolute differences may warrant similar coastal flood risk management responses. For instance, for New York City, we estimate the expected number of historical 100 year ESL events per year between a 2.0 °C to a 1.5 °C GMST stabilization is only two times and one time per year, respectively (figure 2).

While these data could be used in support of local probabilistic risk management strategies that intend to reduce current and future exposure and vulnerability to extreme flood events, some caveats should be highlighted. First, while our projections carry probabilities, these are not uniquely identifiable probabilities; ice sheet contributions in particular are deeply uncertain, so unique probability distributions for their future values do not exist (e.g. Kopp *et al* 2017). Moreover, our projections assume linear accelerations of ice-sheet contributions. Detailed physical models (e.g. Deconto and Pollard 2016) suggest that these approximations may fail over the course of the next three centuries. Rates of ice-sheet contributions may stabilize, or they may cross critical thresholds leading to non-linear accelerations. While the results of Deconto and Pollard (2016) suggest a critical threshold above 2 °C leading to considerably larger Antarctic contributions than at lower temperatures, estimates of the existence, location, and consequences of such thresholds are deeply uncertain. Second, we assume that the frequency of storm arrivals and their intensity will remain constant—and thus the Poisson and GPD parameters (section 2.4.1). Changes to storm frequency and severity could significantly influence future ESL events (e.g. Reed *et al* 2015, Emanuel 2013, Knutson *et al* 2010). Modifications could be made to include changes in these parameters with time (Ceres *et al* 2017). Third, these are projections of extreme high water at specific tide gauges and are not regional flood projections. Future flood projections are dependent on the dynamics of flood propagation, wave action, and future measures taken to reduce flood risk.

The selection of the level at which to stabilize the GMST in the coming years will determine the committed amounts of future GMSL (Clark *et al* 2016, Levermann *et al* 2013). Our projected coastal ESL impacts through the end of the 22nd century should be placed in the context of longer timeframes. Stabilization of GMST does not imply stabilization of GMSL. Regardless of the mitigation scenario chosen, GMSL rise due to thermal expansion is expected to continue for centuries to millennia. Additionally, some studies suggest that sustained GMST warming above given thresholds, potentially those as low as 1 °C, could lead to a near-complete loss of the GIS over a millennium or more (Robinson *et al* 2012). Coincident with continued GMSL rise will be further increases in the frequency of historical ESL events and an increasing number of currently inhabited lands that will be permanently submerged. A comprehensive approach to managing coastal flood risks would take into account changes on these very long timeframes.

Acknowledgments

We are grateful for comments from two anonymous reviewers and Carl-Friedrich Schleussner and colleagues at Climate Analytics. DJR and MKB were supported by the Science, Technology, and Environmental Policy (STEP) Program at Princeton. MO was supported in part by NSF EAR-1520683. REK was supported in part by a grant from Rhodium Group (for whom he has previously worked as a consultant), as part of the Climate Impact Lab consortium, and in part by NSF grant ICER-1663807 and by NASA grant 80NSSC17K0698. We acknowledge the World Climate Research Programme's Working Group on Coupled Modeling, which is responsible for CMIP, and we thank the climate modeling groups for producing and making available their model output (listed in SI table S-2). For CMIP, the US Department of Energy's Program for Climate Model Diagnosis and Intercomparison provides coordinating support and led development of software infrastructure in partnership with the Global Organization for Earth System Science Portals. Code for generating sea-level projections is available in the ProjectSL (https://github.com/bobkopp/ProjectSL), LocalizeSL (https://github.com/bobkopp/LocalizeSL),

and SESL (https://github.com/bobkopp/SESL) repositories on Github. Code for generating extreme sea level projections is available in the hawaiiSL_process (https://github.com/dmr2/hawaiiSL_process), GPDfit (https://github.com/dmr2/GPDfit), return_curves (https://github.com/dmr2/return_curves), and amplification (https://github.com/dmr2/amplification) repositories on Github. The statements, findings, conclusions, and recommendations are those of the authors and do not necessarily reflect the views of the funding agencies.

ORCID iDs

D J Rasmussen https://orcid.org/0000-0003-4668-5749
Maya K Buchanan https://orcid.org/0000-0001-9806-1132
Klaus Bittermann https://orcid.org/0000-0002-8251-6339
Benjamin H Strauss https://orcid.org/0000-0002-6856-6575
Robert E Kopp https://orcid.org/0000-0003-4016-9428
Michael Oppenheimer http://orcid.org/0000-0002-9708-5914

References

Bamber J L and Aspinall W P 2013 An expert judgement assessment of future sea level rise from the ice sheets *Nat. Clim. Change* **3** 424–7
Bittermann K, Rahmstorf S, Kopp R E and Kemp A C 2017 Global mean sea-level rise in a world agreed upon in Paris *Environ. Res. Lett.* **12** 124
Bright E A, Coleman P R, Rose A N and Urban M L 2011 LandScan 2010 Data Set
Buchanan M K, Kopp R E, Oppenheimer M and Tebaldi C 2016 Allowances for evolving coastal flood risk under uncertain local sea-level rise *Clim. Change* **137** 347–62
Buchanan M K, Oppenheimer M and Kopp R E 2017 Amplification of flood frequencies with local sea level rise and emerging flood regimes *Environ. Res. Lett.* **064009** 7
Caldwell P C, Merrifield M A and Thompson P R 2015 Sea level measured by tide gauges from global oceans—the Joint Archive for Sea Level holdings (NCEI Accession 0019568). NOAA National Centers for Environmental Information Dataset
Ceres R L, Forest C E and Keller K 2017 Understanding the detectability of potential changes to the 100 year peak storm surge *Clim. Change* **145** 221–35
Church J *et al* 2013 Sea level change *Clim. Chang. 2013 Phys. Sci. Basis. Contrib. Work. Gr. I to Fifth Assess. Rep. Intergov. Panel Clim. Change* ed T Stocker *et al* (Cambridge: Cambridge University Press) ch 13
Clark P U 2016 Consequences of twenty-first-century policy for multi-millennial climate and sea-level change *Nat. Clim. Change* **6** 360–9
Coles S 2001a Classical extreme value theory and models *Lecture Notes in Control and Information Sciences* (Berlin: Springer) ch 3
Coles S 2001b Threshold models *Lecture Notes in Control and Information Sciences* (Berlin: Springer) ch 4
Deconto R M and Pollard D 2016 Contribution of Antarctica to past and future sea-level rise *Nature* **531** 591–7
Diaz D B 2016 Estimating global damages from sea level rise with the coastal impact and adaptation model (ciam) *Clim. Change* **137** 143–56
Emanuel K A 2013 Downscaling CMIP5 climate models shows increased tropical cyclone activity over the st century *Proc. Natl Acad. Sci. USA* **110** 12219–24
Farrell W E and Clark J A 1976 On postglacial sea level *Geophys. J. R. Astron. Soc.* **46** 647–67
GISSTEMP Team 2017 GISS Surface Temperature Analysis (GISTEMP) (https://data.giss.nasa.gov/gistemp/)
Hansen J, Ruedy R, Sato M and Lo K 2010 Global surface temperature change *Rev. Geophys.* **48** rG4004
Held I M *et al* 2010 Probing the fast and slow components of global warming by returning abruptly to preindustrial forcing *J. Clim.* **23** 2418–27
Hijmans R 2012 GADM database of Global Administrative Areas 2.0 Data Set
Hinkel J *et al* 2014 Coastal flood damage and adaptation costs under 21st century sea-level rise *Proc. Natl Acad. Sci.* **111** 3292–7
Hsiang S *et al* 2017 Estimating economic damage from climate change in the United States *Science* **356** 1362–9
Hunter J 2012 A simple technique for estimating an allowance for uncertain sea-level rise *Clim. Change* **113** 239–52
Jackson L P, Grinsted A and Jevrejeva S 2018 21st century sea-level rise in line with the Paris accord *Earth's Future* **6** 2017EF000688
Jevrejeva S, Jackson L P, Riva R E M, Grinsted A and Moore J C 2016 Coastal sea level rise with warming above 2 °C *Proc. Natl Acad. Sci.* **113** 13342–7
Knutson T R *et al* 2010 Tropical cyclones and climate change *Nat. Geosci.* **3** 157–63
Kopp R E *et al* 2014 Probabilistic 21st and 22nd century sea-level projections at a global network of tide-gauge sites *Earth's Future* **2** 383–407
Kopp R E *et al* 2016a Temperature-driven global sea-level variability in the common Era *Proc. Natl Acad. Sci.* **113** E1434–41
Kopp R E, Shwom R L, Wagner G and Yuan J 2016b Tipping elements and climate–economic shocks: pathways toward integrated assessment *Earth's Future* **4** 346–72
Kopp R E *et al* 2017 Evolving understanding of antarctic ice-sheet physics and ambiguity in probabilistic sea-level projections **5** *Earth's Future* 2017EF000663
Kuhlbrodt T and Gregory J M 2012 Ocean heat uptake and its consequences for the magnitude of sea level rise and climate change *Geophys. Res. Lett.* **39** 1–6
Levermann A, Griesel A, Hofmann M, Montoya M and Rahmstorf S 2005 Dynamic sea level changes following changes in the thermohaline circulation *Clim. Dyn.* **24** 347–54
Levermann A *et al* 2013 The multimillennial sea-level commitment of global warming *Proc. Natl Acad. Sci* **110** 13745–50
Mann M E *et al* 2009 Global signatures and dynamical origins of the little ice age and medieval climate anomaly *Science* **326** 1256–60
Marzeion B and Levermann A 2014 Loss of cultural world heritage and currently inhabited places to sea-level rise *Environ. Res. Lett.* **9** 034
Marzeion B, Jarosch A H and Hofer M 2012 Past and future sea-level change from the surface mass balance of glaciers *Cryosphere* **6** 1295–322
Meinshausen M, Raper S C B and Wigley T M L 2011a Emulating coupled atmosphere-ocean and carbon cycle models with a simpler model, magicc6—part 1: Model description and calibration *Atmos. Chem. Phys.* **11** 1417–56
Meinshausen M *et al* 2011b The {RCP} greenhouse gas concentrations and their extensions from 1765–2300 *Clim. Change* **109** 213–41
Milne G A, Gehrels W R, Hughes C W and Tamisiea M E 2009 Identifying the causes of sea-level change *Nat. Publ. Gr.* **2** 471–8
Mitchell D *et al* 2017 Half a degree additional warming, prognosis and projected impacts (HAPPI): background and experimental design *Geosci. Model Dev.* **10** 571–83

Mitrovica J X *et al* 2011 On the robustness of predictions of sea level fingerprints *Geophys. J. Int.* **187** 729–42
Mohammed K *et al* 2017 Extreme flows and water availability of the Brahmaputra river under 1.5 °C and 2 °C global warming scenarios *Clim. Change* **145** 159–75
Moss R H *et al* 2010 The next generation of scenarios for climate change research and assessment *Nature* **463** 747–56
NASA JPL 2013 NASA Shuttle Radar Topography Mission Global 1 arc second [Data set] NASA LP DAAC
Neumann B, Vafeidis A T, Zimmermann J and Nicholls R J 2015 Future coastal population growth and exposure to sea-level rise and coastal flooding—a global assessment *PLoS ONE* **10**
Perrette M, Landerer F, Riva R, Frieler K and Meinshausen M 2013 A scaling approach to project regional sea level rise and its uncertainties *Earth Syst. Dyn.* **4** 11–29
Rahmstorf S 2007 A semi-empirical approach to projecting future sea-level rise *Science* **315** 368–70
Rahmstorf S, Perrette M and Vermeer M 2012 Testing the robustness of semi-empirical sea level projections *Clim. Dyn.* **39** 861–75
Raper S C B, Gregory J M and Stouffer R J 2002 The role of climate sensitivity and ocean heat uptake on AOGCM transient temperature response *J. Clim.* **15** 124–30
Rasmussen D J, Meinshausen M and Kopp R E 2016 Probability-weighted ensembles of US county-level climate projections for climate risk analysis *J. Appl. Meteorol. Climatol.* **55** 2301–22
Reed A J *et al* 2015 Increased threat of tropical cyclones and coastal flooding to New York City during the anthropogenic era *Proc. Natl Acad. Sci.* **112** 12610–5
Robinson A, Calov R and Ganopolski A 2012 Multistability and critical thresholds of the greenland ice sheet *Nat. Clim. Change* **2** 429–32
Schaeffer M, Hare W, Rahmstorf S and Vermeer M 2012 Long-term sea-level rise implied by 1.5 °C and 2 °C warming levels *Pro. Natl Acad. Sci.* **2** 867–70
Schleussner C F *et al* 2016a Differential climate impacts for policy-relevant limits to global warming: the case of 1.5 °C and 2 °C *Earth Syst. Dyn.* **7** 327–51
Schleussner C F *et al* 2016b Science and policy characteristics of the Paris agreement temperature goal *Nat. Clim. Change* **6** 827–35
Strauss B H, Kulp S and Levermann A 2015 Mapping choices: carbon, climate, and rising seas, our global legacy *Climate Central Report* pp 1–38
Sweet W V and Park J 2014 From the extreme to the mean: Acceleration and tipping points of coastal inundation from sea level rise *Earth's Future* **2** 579–600
Taylor K E, Stouffer R J and Meehl G A 2012 An overview of CMIP5 and the experiment design *Bull. Am. Meteorol. Soc.* **93** 485–98
Tebaldi C, Strauss B H and Zervas C E 2012 Modelling sea level rise impacts on storm surges along US coasts *Environ. Res. Lett.* **7** 14–32
UNFCCC 1992 *The United Nations Framework Convention on Climate Change* (New York: United Nations)
UNFCCC 2015a *Report of the Conference of the Parties on Its Twenty-First Session, Held in Paris from 30 November–13 December 2015* (New York: United Nations)
UNFCCC 2015b *Report on the Structured Expert Dialogue on the 2013-2015 Review* (New York: United Nations)
Vermeer M and Rahmstorf S 2009 Global sea level linked to global temperature *Proc. Natl Acad. Sci.* **106** 21527–32
van Vuuren D P *et al* 2011 The representative concentration pathways: an overview *Clim. Change* **109** 5
Wahl T *et al* 2017 Understanding extreme sea levels for broad-scale coastal impact and adaptation analysis *Nat. Commun.* **8** 16075
Wong P P *et al* 2014 *Coastal Systems and Low-Lying Areas* (Cambridge: Cambridge University Press) pp 361–409